JOURNAL OF MECHANICAL ENGINEERING AND SCIENCES
ISSN: 2289-4659 e-ISSN: 2231-8380
VOLUME 19, ISSUE 1, 2025, 10530 - 10543
DOI: https://doi.org/10.15282/jmes.19.1.2025.8.0825

RESEARCH ARTICLE

Development of an energy-efficient hybrid electric vehicle air-conditioning system test rig coupled with nanolubricant

J. Muriban[1,5], R. Mamat[2]*, G. S. Prayogo[1,3], M. F. Jamlos[4]

[1] Faculty of Technology Mechanical and Automotive Engineering, Universiti Malaysia Pahang Al-Sultan Abdullah, 26600 Pekan, Pahang, Malaysia
[2] Centre for Automotive Engineering, Universiti Malaysia Pahang Al-Sultan Abdullah, 26600 Pekan, Pahang, Malaysia
Phone: +6094316250, Fax.: +6094246345
[3] Department of Mechanical Engineering, Politeknik Negeri Banyuwangi, 68461, Indonesia
[4] Faculty of Electrical and Electronics Engineering Technology, Universiti Malaysia Pahang Al-Sultan Abdullah, 26600 Pekan, Pahang, Malaysia
[5] Centre for Research and Innovation, Jabatan Pendidikan Politeknik dan Kolej Komuniti, 62100 Putrajaya, Malaysia

ABSTRACT - The development of an energy-efficient electric automotive air conditioning system is crucial in addressing the growing concerns over energy consumption and environmental impact in the transportation sector. Prior to assessing the impact of nanolubricants on energy consumption and performance enhancement, a hybrid electric vehicle air conditioning system test rig was developed. Hence, this study focuses on the research and development of an innovative air-conditioning system that incorporates nanolubricants to improve efficiency, thereby reducing overall energy consumption and emissions. The Al_2O_3/POE nanolubricant was synthesized using a two-step method with a volume concentration of 0.15%. The performance of the hybrid electric vehicle air-conditioning system was evaluated based on its cooling capacity and power consumption. The results indicated that compressor work and power consumption were reduced by up to 21.23% and 36.36%, respectively. Based on these findings, a 0.15 vol.% Al_2O_3/POE nanolubricant, combined with a 350 g initial refrigerant charge, was determined to be optimal for performance enhancement and power consumption reduction. The findings of this study have provided significant insights into the potential of nanolubricants to enhance the performance of electrically driven compressor (EDC) air-conditioning systems in hybrid and electric vehicles while reducing energy consumption at various operating speeds.

ARTICLE HISTORY
Received : 18th Oct. 2024
Revised : 20th Feb. 2025
Accepted : 03rd Mar. 2025
Published : 30th Mar. 2025

KEYWORDS
Nanolubricants
Electric compressor
Automotive air conditioning
Hybrid electric vehicle
Aluminium oxide

1. INTRODUCTION

The increasing demand for energy-efficient solutions, particularly in heating, ventilation, and air-conditioning fields, has led to extensive research and technological advancements. The widespread implementation of green and energy conservation policies by government authorities has further encouraged industries to explore innovative materials and technologies [1]. With the rapid transition to hybrid electric vehicles (HEVs) and electric vehicles (EVs), optimizing the performance of electrically driven compressors in automotive air-conditioning systems has become essential [2]. Worldwide energy consumption has consistently increased in recent decades, driven by technological advancements, particularly in the transportation industry [3]. According to research published by the International Energy Agency (IEA) [4], improvements in automotive air-conditioning (AAC) systems can be achieved through active methods such as mechanical and electrical component innovations, powertrain optimization, and cooling load reduction. These combined enhancements have been reported to result in energy savings of up to 36% to 67%, significantly improving vehicle efficiency. Nonetheless, these methods also exhibit specific limitations that need consideration. Active methods can lead to increased complexity and higher initial costs [5]. In recent years, the use of nanolubricants has attracted significant attention in improving the energy efficiency of refrigeration and air conditioning systems. Reviews have demonstrated that nanolubricants improve thermal conductivity, reduce compressor work, and ultimately lower power consumption [6, 7]. Research highlights how nanoparticles, incorporated into base lubricants can enhance heat transfer, reduce friction, and improve the overall performance of these air conditioning systems [8, 9]. A study by Nadia et al. [10] examined the performance of Al_2O_3-SiO_2/polyalkylene glycol (PAG) hybrid nanolubricants in a belt-driven compressor automotive air conditioning (BDC-AAC) system. The study investigated various composition ratios and discovered that a 60:40 blend resulted in a 16.31% gain in COP and an 18.65% decrease in compressor effort. The enhancement was attributable to the hybrid nanolubricants superior heat transfer and lubrication capabilities. Similarly, Sharif et al. [11] developed a numerical simulation model to analyze the cycling behaviour of BDC-AAC systems using Al_2O_3-SiO_2/PAG nanolubricants and R1234yf refrigerant. Their model, validated with experimental data, showed that employing hybrid nanolubricants resulted in lower power consumption, lower temperature cycling frequency, and greater cooling capacity

*CORRESPONDING AUTHOR | R. Mamat | ✉ rizalman@umpsa.edu.my

than standard lubricants. This study proved the feasibility of hybrid nanolubricants in AAC applications. Another study by Cassim et al. [12] investigated the application of multi-walled carbon nanotube (MWCNT) nanolubricants in mechanical heat pump systems. Their findings demonstrated that the incorporation of 0.55 g/L of MWCNT into polyester-based oil resulted in a 34.6% enhancement in coefficient of performance (COP) and a significant decrease in compressor workload. Further studies on performance, conducted by Dilawar et al. [13] utilizing AI_2O_3 nanoparticles in the base fluid and examining the effects in a conventional AAC system, revealed performance enhancements of 32.6%.

A prior investigation by Zawawi et al. [14] on AAC-EDC system explored the impact of nanolubricants in two separate studies, focusing on different formulations of the nanolubricant. One investigation revealed that SiO_2/polyolester (POE) nanolubricants significantly enhanced system efficiency by reducing compressor work by 26.17% and EDC power consumption by 11.97% at a 160 g refrigerant charge. The highest COP of 3.36 was recorded at 1860 RPM with the same charge. In a subsequent study, Zawawi et al. [15] examined TiO_2-SiO_2/POE nanolubricants and found that the highest COP of 2.43 was attained at 160 g refrigerant charge and 1860 RPM, whereas increased EDC power consumption correlated with enhanced compressor performance. While these findings highlight the benefits of nanolubricants in improving system efficiency, most hybrid and electric vehicles rely on high-voltage EDC systems for air-conditioning. However, it is associated with drawbacks such as impacting the overall driving range and efficiency of the vehicles due to the power consumption [16, 17]. Given these concerns, further investigation into low-voltage EDC systems is vital to enhance energy efficiency in electric vehicles. Sanden Manufacturing is a leading manufacturer of automotive thermal system components and is regarded as a pioneer in the development of fully electric and low-voltage electric compressors for passenger cars, particularly for hybrid and electric vehicles [18]. The first generation of electric compressors was developed by Sanden in 2009 with an integrated inverter. Following that, in 2011 and 2018, Sanden launched its first 430 V, 24 V, and 48 V compressors, respectively.

Despite the available literature in the field, research on the performance of HEVs and EVs, which are integrated with fully electric air-conditioning compressors utilizing nanolubricants, remains limited. Addressing this gap, the aim of this study is to investigate the application of AI_2O_3 nanoparticles at a volume concentration of 0.15% in POE-based lubricants for a low-voltage electric compressor of the HEV-AC system. The adoption of the volume concentration was based on experimental observations by Nugroho et al. [19], where this concentration consistently outperformed others in terms of cooling capacity, compressor work reduction, and COP improvement. Their study on residential air-conditioning showed that lower concentrations were ineffective, while higher ones, such as 0.2%, increased viscosity and pressure drop, reducing efficiency. Considering their research focused on other systems, these findings suggest that 0.15% could provide similar performance benefits in AAC systems, making it a promising candidate for further evaluation to ensure an optimal balance of stability and thermal performance. The AI_2O_3 nanoparticles were chosen due to their exceptional thermal conductivity properties and stability [20, 21]. Hence, to develop and evaluate the HEV-AC system, a customized test rig was designed and constructed. The study then aimed to assess the cooling capacity and power consumption performance of the system with utilization of the nanolubricants.

2. MATERIAL AND METHODS

2.1 Test Rig Development

The test rig was developed in compliance with American Society of Heating, Refrigerating and Air-Conditioning Engineers (ASHRAE) Standard 41.9 [22, 23], which defines standard methods for refrigerant mass flow measurements using calorimeters. A calorimeter is designed as a thermally insulated instrument and equipped with a heat exchanger to measure the mass flow rate of a volatile refrigerant by assessing the heat input and output corresponding to a specified enthalpy change. According to the standard, calorimeters are classified as either evaporator or condenser calorimeters. And evaporator calorimeters are further categorized into three types: (i) secondary refrigerant calorimeters, (ii) secondary fluid calorimeters, and (iii) primary refrigerant calorimeters. Among these, the secondary fluid calorimeter was employed due to its compatibility for heat exchange measurements with water in this experimental setup.

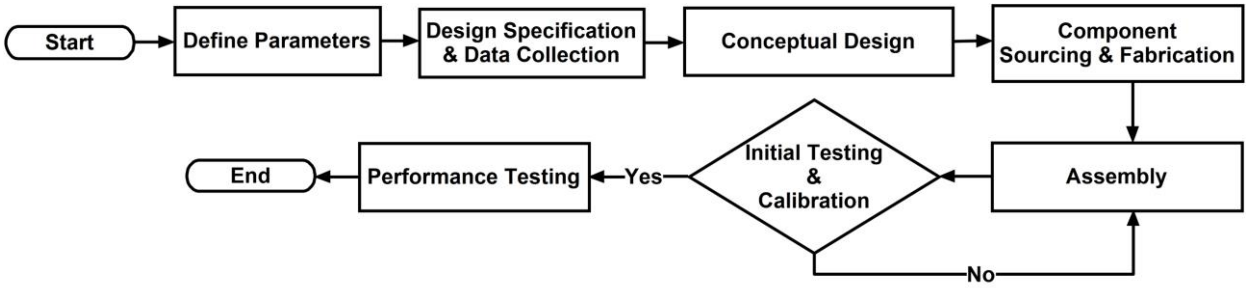

Figure 1. Test rig development flowchart

The development of the HEV air-conditioning system test rig consists of several processes, shown in Figure 1. Initially, defining parameters in the development of the test rig involved defining the essential parameters that influence system performance. These parameters included the operational limits of the HEV-AC system and specific component characteristics required to simulate actual electric automotive conditions in accordance with the standard. Following parameter definition, detailed design specifications were prepared. This phase involved extensive data collection to support design choices, including selection of components, layout considerations, and integration of measurement instruments to ensure comprehensive data capture during testing. With specifications in hand, a conceptual design was developed in computer-aided design (CAD) as displayed in Figure 2. This design provided a blueprint of the test rig layout and component interaction, which is significant for achieving the desired test conditions and ensuring the rig's operational efficacy.

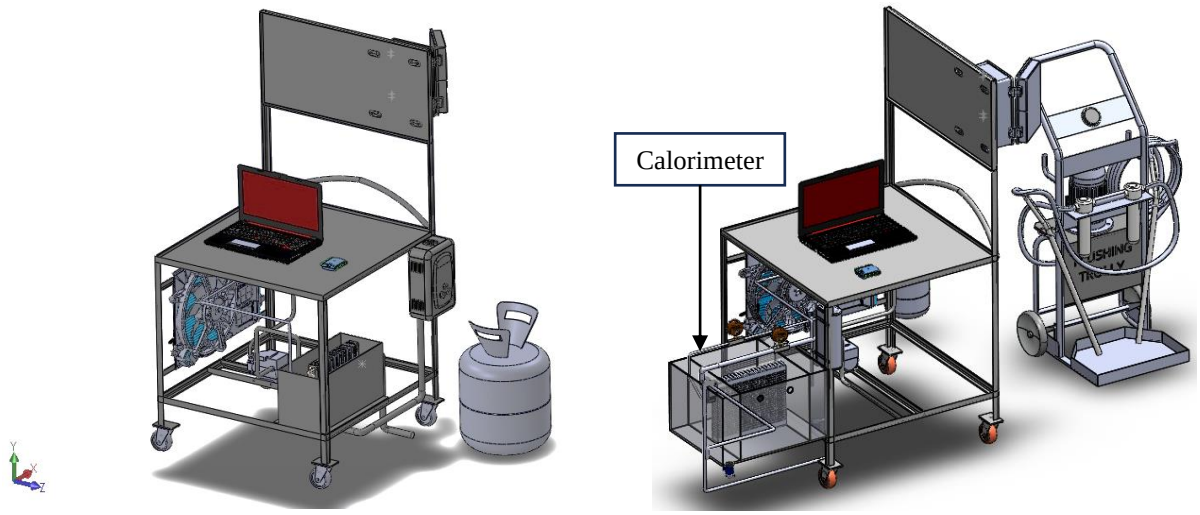

(a) (b)

Figure 2. CAD conceptual design: (a) Preliminary design and (b) Final design

Table 1. List of components of the HEV air conditioning system test rig

No.	Description	No.	Description
1	Evaporator Calorimeter	11	Water inlet from Calorimeter
2	Water Flow Meter	12	Water Pump
3	Calorimeter Outlet	13	High Pressure Service Port/Valve
4	Water Heater Unit	14	High Pressure Pipe (Side)
5	Low Pressure Service Port/Valve	15	Condenser Fan
6	Low Pressure Pipe (Side)	16	Air Duct
7	Electric Compressor (ES18C)	17	Calorimeter Inlet
8	Condenser	18	LCD Display
9	Water Tank (Supply)	19	Control Unit Box (Arduino Assembly)
10	Water outlet from Tank	20	Power Converter

The components listed in Table 1, including the insulated calorimeter, aluminium pipes, and service valves for high pressure (HP) and low pressure (LP), were sourced and fabricated as required. This stage was essential in customizing the HEV air-conditioning system testing to meet specific requirements, such as ensuring compatibility with a simulated car model and adherence to ASHRAE standards. Following this, the components were assembled, with each component meticulously positioned according to the conceptual layout to facilitate maintenance and adjustments. Wiring and plumbing were completed with precision to prevent leaks and electrical faults.

Following this, just before recharging the system with refrigerant, the test rig was flushed, vacuumed, and leak-tested after being fully assembled, as illustrated in the complete procedures shown in Figure 2. The process began with an initial assessment, which included a visual inspection of the mechanical and electrical installation to evaluate the condition of the air conditioning (AC) system. This step was performed to identify any obvious issues or malfunctions requiring immediate attention before proceeding with the system flushing procedures. At this stage, the AC system is manually flushed with nitrogen to remove moisture and clear out any residual impurities that could affect performance or cause corrosion. Once flushing is completed, the system is vacuumed for a duration of 30 minutes [24]. A vacuum pump is used to remove any remaining air or nitrogen in the AC system, creating a vacuum to ensures that no air or non-condensable

gases remain, which could compromise the AC system efficiency and performance also lead to hose degradation and potential system failures. After the vacuum process was completed, the AC compressor was pre-filled with lubricants. However, lubricant levels were inspected as a precautionary measure. This step is crucial, as lack of lubrication may instantly damage the compressor. Prior to system charging, a leak test must be performed for 15 minutes immediately after the system has been vacuumed to detect any immediate leaks.

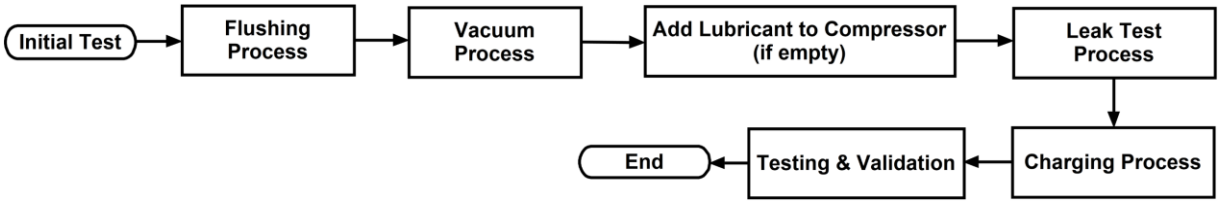

Figure 2. Testing procedures for the HEV-AC test rig

Additionally, the system should be monitored for potential microleaks, which may take several days to become noticeable. Therefore, further leak checks should be conducted the following day to ensure long-term system integrity. Next, the system should be charged with refrigerant. This study, the Universal Scroll-type Electric AC compressor (ES18C) was employed. The test rig installation is carried out with modifications related to mounting and positioning, where the evaporator, condenser, receiver drier, and expansion valve are retrofitted from Denso original equipment manufacturer (OEM) parts. Subsequently, the system is retrofitted with a speed adjustable electric driven compressor, which is controlled by a pulse width modulation (PWM) controller. The refrigerant type and charge amount for the initial test run were determined according to the manufacturer's specifications to ensure optimal system performance. Nevertheless, due to the variations in piping length and system configuration of the newly built HEV air conditioning test rig, the manufacturer's recommended charge quantity may no longer be ideal. The optimal refrigerant charge for the test rig was determined in accordance with the SAE J2765 standard method [25]. Finally, the system is tested and validated to ensure proper functionality.

2.2 Calibration and Installation of Thermocouples

The calibration of sensors and instruments was essential to ensure that data collected was reliable and reflective of actual performance. Figure 4 illustrates the test rig schematic diagram, which details the exact locations of all sensors. The temperature is measured and monitored using thermocouples connected to a data logger. Pressure manifold gauge is utilized to measure and track the pressure levels within the refrigeration system. In addition, a flow meter is employed to ensure the consistent movement or flow of water from the heater, while a vibration sensor is used to assess the displacement of the compressor. Furthermore, Kyoritsu KEW6310 power analyzer and an AC/DC power clamp is utilized to monitor the power consumption of an electrically driven compressor. Sensors are positioned at the key components of the AC system to monitor and record system performance. The collected data is then evaluated to determine energy consumption, cooling rate capacity, and compressor work. Section 3 presents the analyzed data findings.

Table 2. Calibration data for thermocouples [26, 27]

Thermometer Reference	Freezing	Boiling	
Platinum (SPRT)	0 (℃)	100 (℃)	
K type Thermocouple	Temperature Measurement (℃)		Description (Location Point)
T_1	0.21	100.00	Comp. inlet
T_2	0.88	99.87	Comp. outlet
T_3	0.60	100.10	Cond. inlet
T_4	0.54	99.88	Cond. outlet
T_5	0.61	99.98	Liquid line
T_6	0.55	99.70	TXV inlet
T_7	0.23	99.83	TXV outlet
T_8	0.66	99.72	Calorimeter inlet
T_9	0.63	99.87	Evap. outlet
T_{10}	0.08	100.00	Evap. inlet
T_{11}	0.51	99.91	Calorimeter outlet
T_{12}	0.19	100.00	Water outlet temp.1
T_{13}	0.75	100.10	Water outlet temp.2
T_{14}	0.63	99.91	Water inlet temp.1
T_{15}	-0.10	100.00	Water inlet temp.2

Prior to installation, each thermocouple was calibrated using a platinum thermocouple against the freezing and boiling points of water. Furthermore, three pressure points were installed on the pipes that were connected to both the high pressure and low-pressure lines of the system. Table 2 shows a set of data referring to the water conditions used for calibration. The K-type thermocouples have a diameter of 0.3 mm and are designed for a temperature range of −40 ℃ to 400 ℃, with a tolerance of ±1.5 ℃. All thermocouples were calibrated to ensure measurement accuracy.

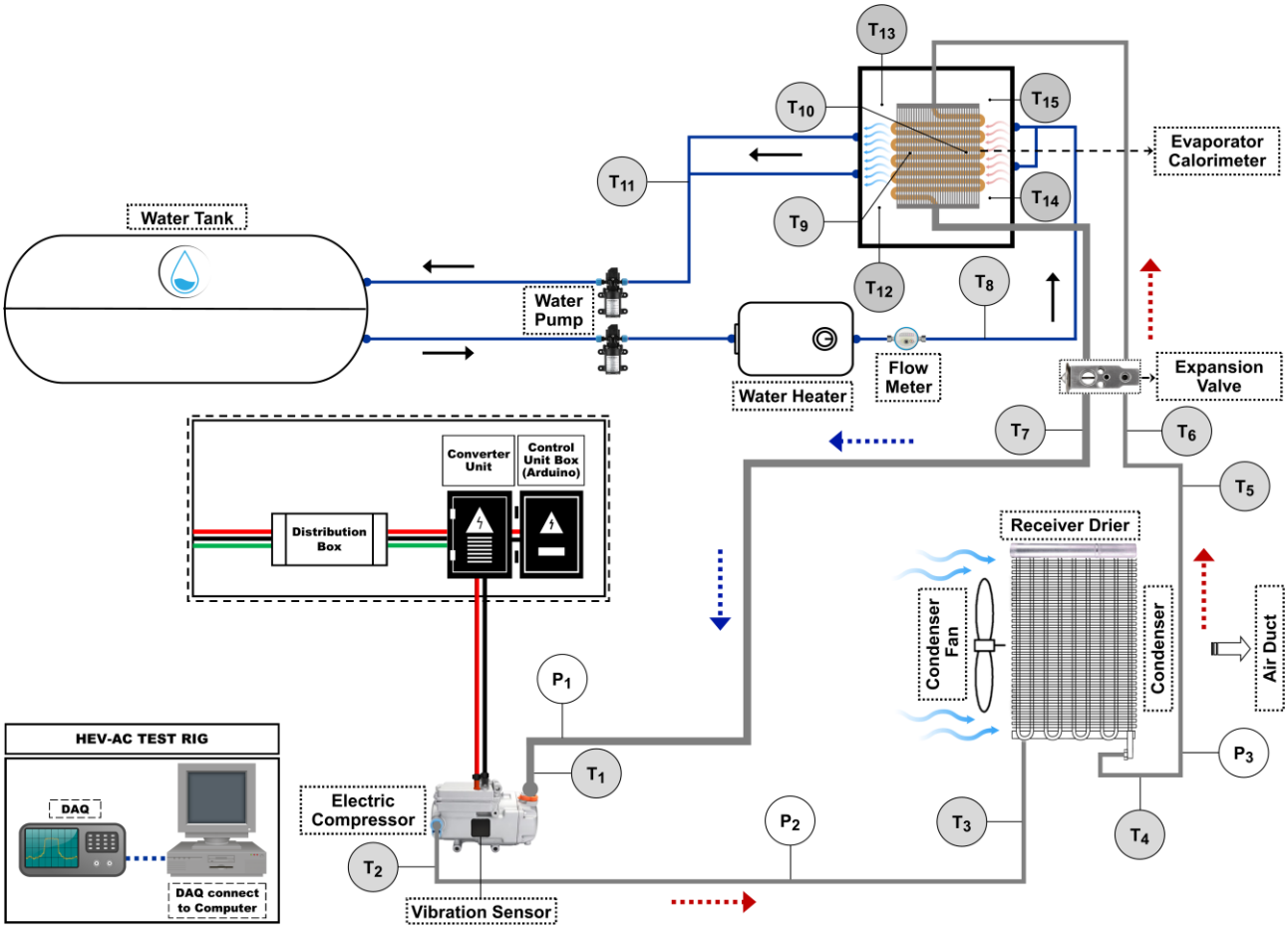

Figure 4. The schematic diagram of HEV-AC system with thermocouples and pressure points

2.3 Performance Analysis of the System

The efficiency of the HEV air-conditioning system was assessed based on energy consumption, cooling rate capacity, and compressor work. According to the Society of Automotive Engineers (SAE) standard for measuring system performance SAE-J2765 [25], the testing facility has two types of benches: enclosed and open bench, with specific spaces for testing condensers and evaporators. This present work, an open bench is adopted, typically for open bench the components and sections such as the evaporator and condenser test sections are more open to the surrounding environment. Nevertheless, the test rig for these experiments has been situated in a control room. The temperature of the room monitored and controlled between 33 ℃ to 35 ℃. The test room methods need the allocation of different rooms for vehicle components to replicate the actual condition of the vehicle, with the evaporator located in the car room and the compressor and condenser in the under-hood room conditions. As the standard suggested approach for testing in variation of specified compressor speeds is to perform test experiments under L35a conditions [25], compressor speeds can be easily modified to accommodate different drive ratios or compressor types, ensuring that the RPM matches the system capacity. Based on the L35a test conditions, the evaporator temperatures should be maintained at 35 ℃, air mass flow at 9 kg/min is simulated with air selection under open outside air (OSA) and humidity at 40%. However, in the current test rig configuration, an immersion evaporator is incorporated into the calorimeter, which leads to substitutions in the standard test conditions. As a result, certain aspects of the L35a test standard are not strictly applied. Instead, the evaporator conditions are established based on recognized standards for calorimeter test methods for volatile refrigerants, as shown in Figure 5.

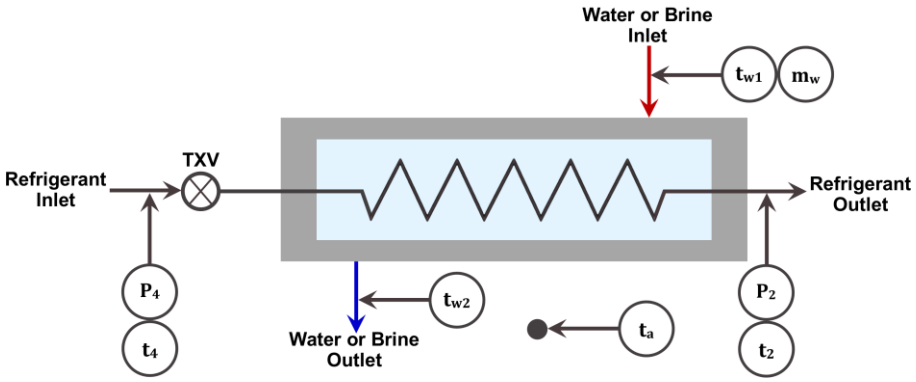

Figure 5. Secondary fluid calorimeter

Figure 6 depicted the real cycle of the Temperature-Entropy (T-s) diagram for R134a employed with POE. various processes within the cycle are marked by state changes from T_1 through T_8, each representing critical transitions in the refrigeration process. During the isentropic compression phase from T_1 to T_2, the refrigerant, initially in a low-pressure and low-temperature vapor state at T_1, is compressed by the compressor. This process is adiabatic, meaning no heat is exchanged with the environment, leading to an increase in both temperature and pressure of the refrigerant without a change in entropy. The work done by the compressor on the refrigerant increases its internal energy and prepares it for the heat rejection phase. From T_3 to T_4, the superheated vapor then enters the condenser where it releases heat to the surroundings and changes into a saturated liquid. This process results in a significant drop in temperature while the entropy decreases, reflecting the loss of heat. The throttling process from T_5 to T_6 occurs in an expansion device, such as a capillary tube or expansion valve, where the refrigerant experiences a pressure drop without significant heat transfer or work input/output. This results in a decrease in both pressure and temperature but occurs at nearly constant enthalpy. Throttling is essentially an isenthalpic process (constant enthalpy), leading to a reduction in temperature as the refrigerant enters the evaporator. Finally, from T_7 to T_8, the low-pressure liquid refrigerant absorbs heat from the environment in the evaporator, causing it to evaporate. This phase change occurs at constant pressure and results in an increase in both entropy and temperature as the refrigerant takes in thermal energy, which turns it back into a vapor. This heat absorption process is critical as it enables the refrigerant to extract heat from the refrigerated environment, thereby cooling it [28]. Precise temperature and pressure measurements are essential at specific locations and conditions to evaluate compressor operation, system power consumption, cooling capacity, and coefficient of performance. The compressor power consumption, $\dot{W}_{in}$ is determined by Eq. (1), the power consumed by the electric AAC system, P by Eq. (2), and the reduction in power consumption, $E_{reduction}$ by Eq. (3) , while maintaining a water mass flow rate of 4.5–5 LPM and a specific heat capacity of the water, $C_{p,water}$ is 4.18 kJ/kg·°C, which value obtained from [28]. The cooling capacity rate, $\dot{Q}_L$ is then calculated using Eq. (7).

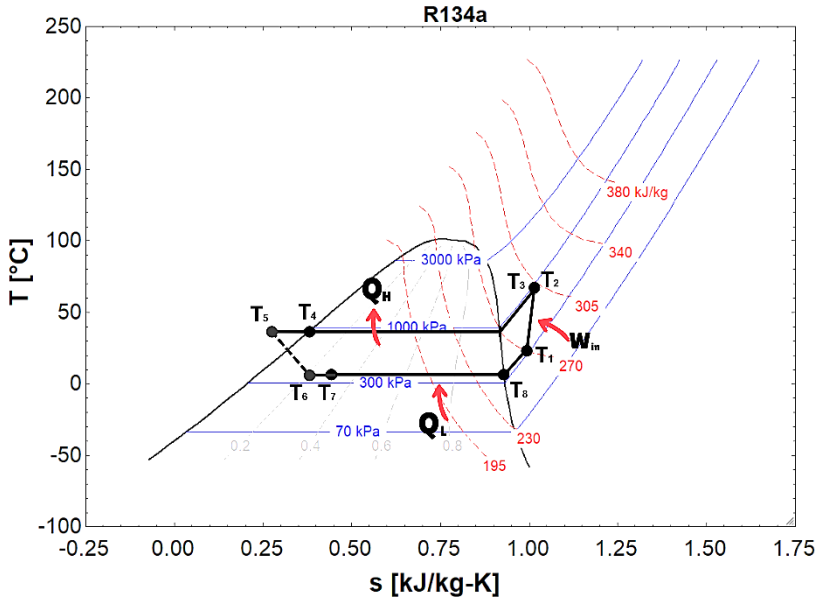

Figure 6. T-S diagram of the actual cycle of HEV-AC syste

From Eq. (1), the power consumption of the compressor at a given moment is where, $\dot{m}$ is the mass flow rate of the refrigerant and $(h_2 - h_1)$ is the change in enthalpy of the refrigerant through the compressor. In Eq. (2), this equation

determines the total electrical power consumed by the HEV air conditioning system. The enthalpy-based method, $\dot{W}_{in}$ assesses compressor performance and efficiency from a thermodynamic perspective, while the electrical method, P is crucial for designing electrical systems evaluating overall system efficiency, integrating both electrical and mechanical factors.

$$\dot{W}_{in} = \dot{m}(h_2 - h_1) \tag{1}$$

$$P = IV \tag{2}$$

The Eq. (3) derived the percentage reduction in power consumption between a compressor utilizing pure lubricant and one employing a nanolubricant. $\dot{W}_{Pure\ Lub.}$ is the power consumption with pure lubricant, and $\dot{W}_{NL}$ is the power consumption with nanolubricant.

$$E_{reduction} = \frac{\dot{W}_{Pure\ Lub.} - \dot{W}_{NL}}{\dot{W}_{Pure\ Lub.}} \times 100\% \tag{3}$$

As Eq. (4) defines ΔT as the difference between the average inlet and outlet temperatures of the calorimeter [23].

$$\Delta T = \text{Avg. inlet water bath temp.} - \text{Avg. oulet water bath temp.} \tag{4}$$

The average temperature, c of the water, calculated using the temperatures at two different points t_{w1} and t_{w2} by Eq. (5).

$$c = \frac{t_{w1} + t_{w2}}{2} \tag{5}$$

Eq. (6) is used to calculate the mass flow rate of the refrigerant [23]. The m_w represents the water mass flow rate, $t_{w1} - t_{w2}$ is the change in water temperature, q_a represents any additional heat added to or lost from the system, and $h_2 - h_1$ calculates the change in enthalpy of the refrigerant as it moves through the compressor, encapsulating the energy transformation within the system.

$$m = \frac{[m_w c(t_{w1} - t_{w2}) + q_a]}{(h_2 - h_1)} \tag{6}$$

Cooling capacity rate, $\dot{Q}_L$ calculated based on Eq. (7), $\dot{m}_w$ is the mass flow rate of the water, $C_{p,water}$ is the specific heat capacity of water and ΔT is the temperature difference across the calorimeter component [28].

$$\dot{Q}_L = \dot{Q}_{water} = \dot{m}_w C_{p,water} \Delta T \tag{7}$$

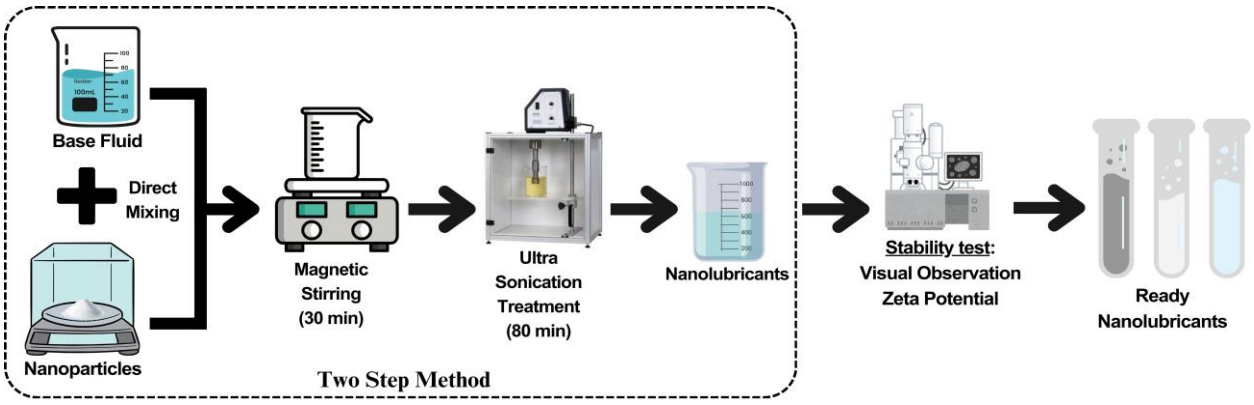

Figure 7. Two-step method for synthesizing nanolubricants

2.4 Nanolubricant Preparation

The nanolubricant in this work were synthesized through a two-step method [29], which illustrated in Figure 7. Within this experiment, the nanoparticles employed are AI_2O_3 and the base fluid is Polyolester. Initially, AI_2O_3 nanoparticles were dispersed into POE lubricant and mixed using an INTLLAB Magnetic Stirrer at 3000 RPM for 30 minutes, followed by sonication in a Hielscher Ultrasonics UP400S homogenizer for 80 minutes to ensure a uniform distribution and prevent particle aggregation as suggested by Nugroho et al. [30]. The volume concentrations of the nanolubricant were determined by Eq. (8), which calculates the percentage based on the mass and density of the nanoparticles and the base lubricant. Following synthesis, stability measurements were conducted to assess the suspension stability of the nanoparticles over time, ensuring the long-term efficacy of the nanolubricant.

$$\phi = \frac{\frac{m_{np}}{\rho_{np}}}{\frac{m_{np}}{\rho_{np}} + \frac{m_{bl}}{\rho_{bl}}} \times 100 \quad (8)$$

2.5 Experimental Procedures

The HEV air conditioning system for the experimental setup was charged with R134a refrigerant, with an initial charge of 250 to 400 grams. This range allows for a more in-depth analysis of the system operating efficiency by examining its performance at various refrigerant charge levels. SAE standards were adhered to during the testing processes [25]. The test rig was operated for a minimum of 20 minutes to ensure that the system reached a steady state condition. The data was then recorded for 10 minutes. Each set of data was collected three times on different days to ensure that the measurement is reliable and precise. The system was tested using both traditional lubricants and nanolubricants, with the performance of the system under various operating conditions being evaluated. Table 3 shows the test parameters employed.

Table 3. Test parameters for the HEV-AC system

Parameters	Unit	Range
Compressor Speed	RPM	2000 – 5000
Refrigerant Charge (R-134a)	g	250 – 400
Compressor Lubricant (Volume)	mL	100
Volume Concentration, ϕ	%	0.15
Water Flow Rate (Secondary Fluid Calorimeter)	LPM/minute	4.5 – 5
Front Evap. Temp. (Inlet Fluid of Calorimeter)	℃	35

2.6 Uncertainty and Consistency Analysis

The relative standard error (RSE) method was used for data consistency analysis in examining measurement errors for HEV-AC test rig performance parameters. Various measuring devices and sensors were employed, including thermocouples, refrigerant gauges, flow meters, vibration meters, power analyzers and weighing scales. These instruments provided critical data on key measurement variables such as temperature, pressure, power consumption, vibration and water flow rate. Table 4 provides detailed uncertainty data for each equipment and sensor with values ranging from 0.01% to 4.5%. The RSE measures data reliability by quantifying variation relative to the mean of the sample collection, as shown in Eq. (9), $\bar{X}$ is the mean of the sample collection.

$$RSE = \frac{S_{err}}{\bar{X}} \times 100\% \quad (9)$$

where, S_{err} is the standard error, calculated using Eq. (10),

$$S_{err} = \frac{\sigma}{\sqrt{n}} \quad (10)$$

The standard deviation, σ is obtained by Eq. (11) [31], where X_i represents each individual data point in the sample. The term $(n-1)$ denotes the degrees of freedom and is used instead of n to correct for bias in the sample standard deviation, following Bessel's correction.

$$\sigma = \sqrt{\frac{\sum_{i=1}^{n}(X_i - \bar{X})^2}{n-1}} \quad (11)$$

Table 4. Uncertainty analysis of the measuring instruments

Parameters	Uncertainty (%)
K-type Thermocouple, ℃	±1.29
Pressure Guage, PSI	±0.50
Weighing Scale (DSZH RCS-7040), g	±0.10
Water Flow Meter, L	±0.01
Power Analyzer, W (Kyoritsu KEW6310)	±0.20
Vibration Velocity, mm/s	±4.50

3. RESULTS AND DISCUSSION

3.1 Full Setup of the Hybrid Electric Vehicle Air Conditioning System Test Rig

A newly developed HEV air conditioning test rig has been fully constructed. The rig developed consists of OEM components of the electric compressor, condenser, evaporator, expansion device, and other necessary parts to replicate actual vehicle operating conditions, as shown in Figure 8. The test rig is equipped with the Universal (ES18C) low voltage (12 VDC) Electric Compressor. The compressor is compatible with the Toyota Prius Hybrid 1.5 [32], Honda Velez Hybrid 1.5 and the Honda Jazz 1.5 Hybrid (GP5). Moreover, it is also adaptable for truck campers and truck buses, according to manufacturer manuals.

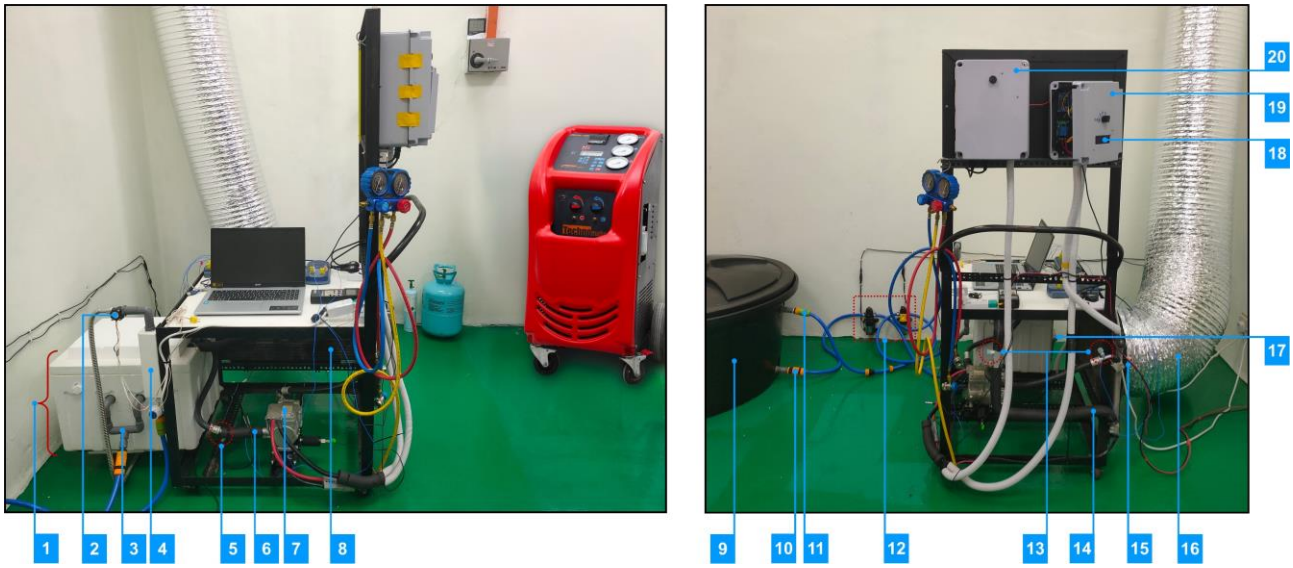

Figure 8. HEV air conditioning system test rig

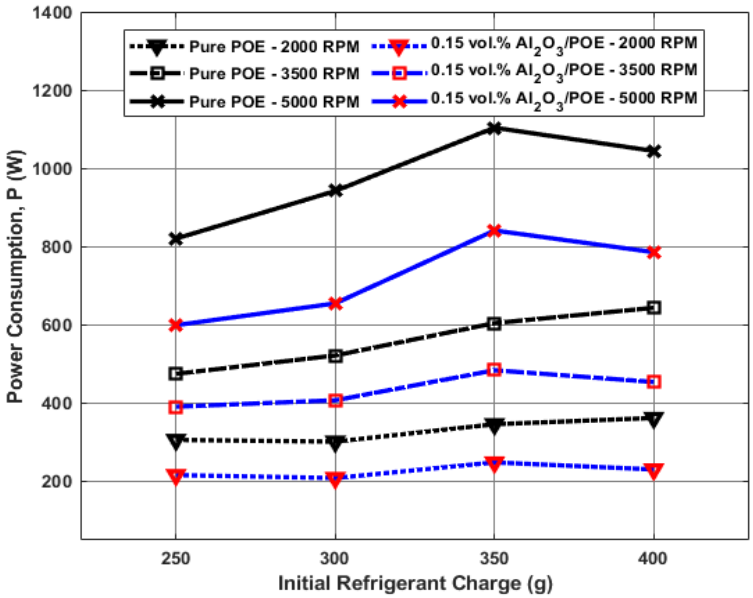

Figure 9. Power consumption of pure POE and nanolubricants with varying initial refrigerant charges

3.2 Consumption Analysis at Various Refrigerant Charge Levels

This section examines the power consumption characteristics of an HEV air conditioning system, focusing on two types of lubricants: conventional polyolester and nanolubricants with a 0.15% concentration of aluminium oxide (AI_2O_3) nanoparticles dispersed in POE. Power consumption from the enthalpy-based method, $\dot{W}_{in}$ is used to assess compressor performance and efficiency from a thermodynamic perspective, while the electrical method, P is crucial for evaluating overall system efficiency by integrating both electrical and mechanical factors. Figure 9 highlights the power consumption, P varies with refrigerant charge (250 g, 300 g, 350 g, 400 g) and compressor speeds (2000 RPM, 3500 RPM, 5000 RPM). At 2000 RPM, power consumption for pure POE increases from 305 W at 250 g to 362 W at 400 g,

reflecting the higher load on the compressor. In contrast, nanolubricants exhibit lower power consumption, starting at 216 W and rising to 230 W, suggesting improved efficiency due to reduced friction and enhanced heat transfer. At 3500 RPM, pure POE power consumption ranges from 474 W to 643 W as refrigerant charge increases. Nanolubricants, however maintain lower power consumption, ranging from 390 W to 453 W. The effectiveness of nanolubricants in reducing power consumption remains evident at this moderate speed, where it continues to mitigate friction and improve system performance. At 5000 RPM, the highest speed, pure POE power consumption rises sharply from 820 W at 250 g to 1044 W at 400 g, indicating significant energy demands at high speeds. Nanolubricants show a lower range, starting at 599 W and increasing to 785 W, demonstrating their efficiency in reducing power consumption under high-speed, high-load conditions. Across all speeds and refrigerant charges, nanolubricants consistently reduced power consumption compared to pure POE, particularly at higher RPMs, where the benefits of reduced friction and enhanced thermal conductivity become more pronounced.

Figure 10 presents the percentage reduction in power consumption, $\dot{W}_{in}$ for the HEV-AC system using pure lubricant compared to one using nanolubricants (AI_2O_3/POE) across different refrigerant charges (250 g to 400 g) and compressor speeds. Above the 0% threshold indicates that the nanolubricant consumes more power than the pure POE lubricant. Below the 0% threshold shows that the nanolubricant consumes less power than the pure POE lubricant. At 250 g, the power reduction at 2000 RPM is minimal, with a reduction consumption of 0.43%. However, as the speed increases to 3500, a significant reduction of 22.69% is observed, and it remains notable at 5000 RPM with 15.33%, indicating that nanolubricants consume considerably less power compared to pure POE. For the 300 g charge, nanolubricants show a 17.97% reduction at 2000 RPM. At 3500 RPM, the reduction is slightly lower at 10.96%, yet it still demonstrates improved efficiency. The trend continues at 5000 RPM, where the power reduction stabilizes at 14.97%, reinforcing the lower energy consumption associated with nanolubricants. At 350 g, the nanolubricants show strong performance, with a power reduction of 18.42% at 2000 RPM, followed by a more significant 21.65% reduction at 3500 RPM. The highest decrease is observed at 5000 RPM, where power consumption is reduced by 29.03%, demonstrating substantial energy savings under high-load conditions.

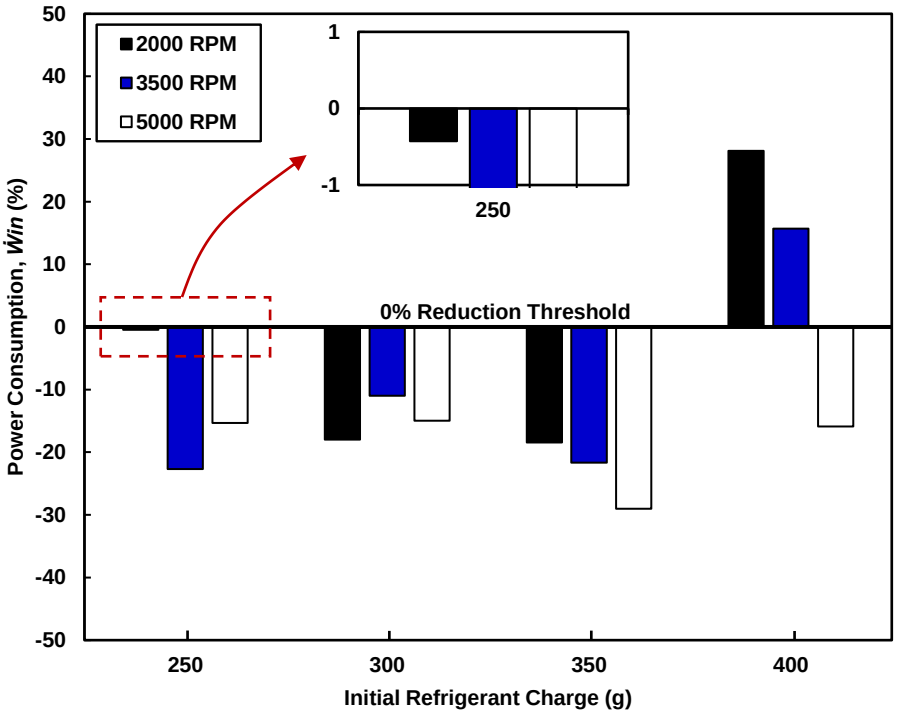

Figure 10. Power consumption reduction (%) at various RPM and initial refrigerant charge levels

For the 400 g charge, the trend shifted. At 2000 RPM, nanolubricants consumed more power above 0% threshold, than pure POE, with a 28.11% increase. A similar result is seen at 3500 RPM, where power consumption increased by 15.68%. The inefficiencies observed at these 400 g refrigerant charge at lower RPMs may result from excessive refrigerant accumulation, leading to increased compression work, reduced heat transfer efficiency, and higher viscous losses. Excessive refrigerant accumulation can lead to suboptimal performance by causing an imbalance in the system's pressure and flow dynamics. This can result in increased energy consumption and reduced cooling efficiency [33]. With excess refrigerant charge, suction and discharge pressures are raised, increasing the pressure ratio and compressor workload while reducing volumetric efficiency. And at lower RPMs, refrigerant circulation is limited by a lower mass flow rate (ṁ), leading to poorer heat absorption in the evaporator and higher condenser saturation, which further strains compressor

performance [28]. However, at 5000 RPM, improved shear forces, greater refrigerant circulation, and enhanced convective heat transfer restore nanolubricant efficiency, reducing compressor power consumption and mitigating frictional losses. Overall, nanolubricants have been shown to provide consistent energy savings at lower refrigerant charges and higher RPMs. However, efficiency is reduced at the highest refrigerant charge (400 g) when operating at lower RPMs. Nonetheless, performance improves at higher RPMs, particularly under heavier load conditions.

3.3 Correlation of the Compressor Work and Power Consumption

Figure 11 shows compressor work and power consumption in a system with nanolubricants across various refrigerant charge levels and compressor speeds. The compressor work represents the change in enthalpy of the refrigerant as it passes through the compressor and serves as a measure of the energy required to circulate the refrigerant throughout the system [28]. The correlation between compressor work and power consumption shows a clear trend across various refrigerant charges and RPM levels. At 250 g of refrigerant charge, the compressor work at 2000 RPM starts at 27.53 kJ/kg, increasing steadily to 62.93 kJ/kg at 5000 RPM. Correspondingly, power consumption at this charge level rises from 216 W at 2000 RPM to 599.16 W at 5000 RPM. This pattern demonstrates that higher RPMs demand more mechanical work, leading to increased electrical power usage. At 300 g, compressor work and power consumption follow a similar trajectory, with work increasing from 22.68 kJ/kg at 2000 RPM to 55.96 kJ/kg at 5000 RPM, and power consumption rising from 208.44 W to 654.84 W. The trend is even more pronounced at 350 g, where compressor work at 5000 RPM reaches 49.04 kJ/kg, while power consumption jumps significantly to 841.20 W. Finally, at 400 g of refrigerant charge, the compressor work at 2000 RPM starts at 23.87 kJ/kg, increasing to 49.88 kJ/kg at 5000 RPM, while power consumption rises from 230.40 W to 785.64 W.

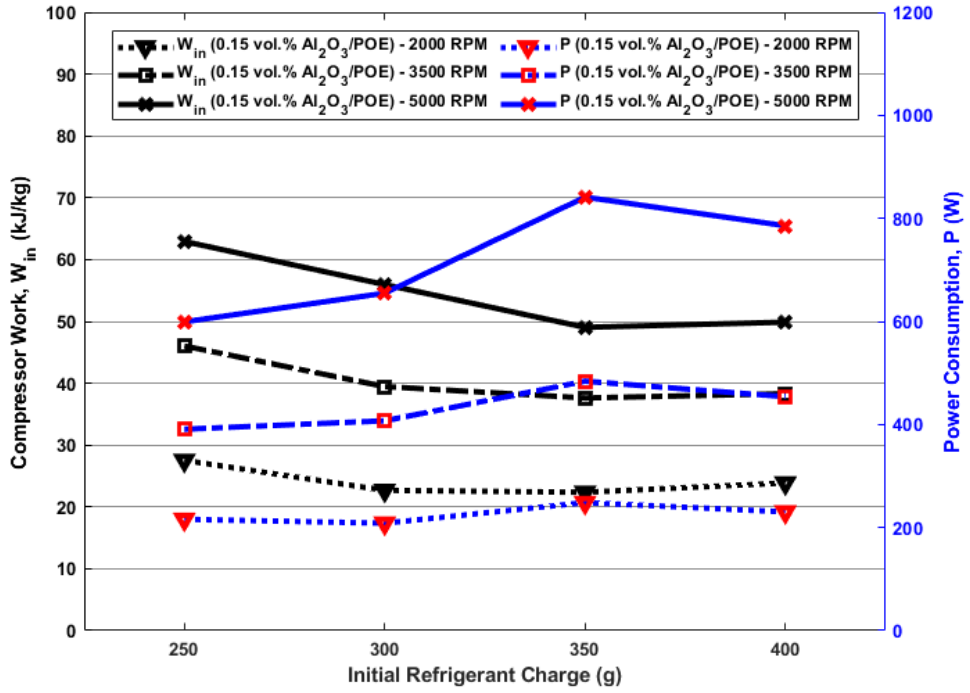

Figure 11. Compressor work and system power consumption against the initial refrigerant charge

Across all charge levels and RPMs, the result clearly shows that as the refrigerant charge and RPM increase, both the compressor work and the corresponding power consumption rise, emphasizing the direct relationship between mechanical and electrical energy demands in the system. Furthermore, based on the specific condition notably the 350 g refrigerant charge, a comparison of all RPMs for compressor work indicates an inverse trend when compared to power consumption for similar refrigerant charges. It decreases with increasing initial refrigerant charge and compressor speed. The inverse trend between compressor work and power consumption as refrigerant charge and compressor speed increase can be attributed to the thermodynamic behaviour of the system and the efficiency of the compressor under different operating conditions [28]. Sharif et al. [34] conducted experiments with traditional belt-driven compressors adopting nanolubricants dispersed in PAG base fluid revealing a similar pattern of the compressor performance against various refrigerant loads.

3.4 Effect of Nanolubricants in HEV-AC System on Cooling Rate Capacity

On the other hand, Figure 12 presents the cooling capacity across multiple initial refrigerant charges for pure polyol ester and nanolubricants with an AI_2O_3 (0.15%) concentration. Across all refrigerant charges and compressor speeds, the system utilizing AI_2O_3 nanolubricants shows consistently higher cooling capacities compared to the system using pure POE. It is the evident that AI_2O_3 nanoparticles enhance lubricant thermal conductivity, enhancing heat exchange between

refrigerant and compressor, increasing cooling capacity, especially at higher speeds and refrigerant charges. In common operating conditions, a small amount of miscible lubricant can evaporate and mix with the refrigerant [35]. The nanolubricants may enhance the refrigerant ability to transfer heat in the evaporator and condenser, contributing to the higher cooling capacities observed across different operating conditions. Additionally, nanolubricants provide improved lubrication within the compressor, reducing frictional losses. This more efficient operation can contribute to higher cooling capacities, as less energy is lost to mechanical inefficiencies, allowing more energy to be used for cooling. The obtained results align with the findings reported by [36-38]. The cooling capacity performance is increasing substantially in a linear manner with the quantity of refrigerant charged. However, the increase in cooling capacity varies partially clearly can be observed in pure POE and there may be diminishing returns as the refrigerant charge approaches the system optimal level. Overcharging the system could lead to inefficiencies.

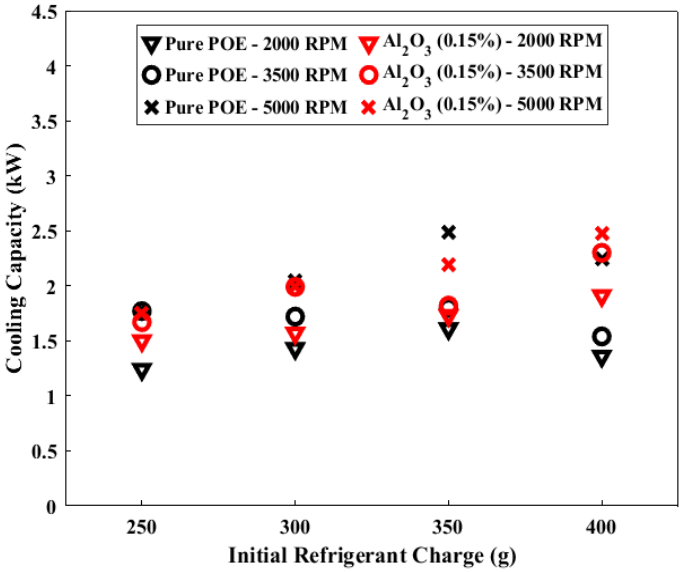

Figure 12. Cooling capacity at various initial refrigerant charge levels

4. CONCLUSIONS

The development of the energy-efficient HEV air conditioning system is extensively described, including the calibration and placement of thermocouples, as clearly illustrated in the schematic diagram. The uncertainties of the experimental parameters have been comprehensively addressed, ensuring accuracy in the analysis. A nanolubricant was synthesized in this work using a two-step method and the Al_2O_3/POE nanolubricants shown exceptional stability as determined by stability assessment. Key aspects of performance such as power consumption, compressor work, and cooling capacity were effectively measured and plotted. With the nanolubricants of 0.15% volume concentration, showed the highest reduction in power consumption, especially at a 350 g refrigerant charge. The compressor work, W_{in} and power consumption, P were reduced by up to 21.23% and 36.36%, respectively, underscoring the improved efficiency of the system using nanolubricants. Therefore, it is recommended that for optimal performance and minimize power consumption of an EDC air conditioning system operating with Al_2O_3/POE nanolubricants is with 350 g refrigerant charge. Future studies are recommended to optimize nanolubricant concentrations and further refine the refrigerant charge range, focusing on 320 g to 380 g to identify the precise conditions for maximum efficiency.

ACKNOWLEDGEMENTS

The authors would like to express their gratitude to Universiti Malaysia Pahang Al-Sultan Abdullah for the financial support provided given under RDU223310 and RDU240703, respectively.

CONFLICT OF INTEREST

The authors disclose no financial or personal interests that could have impacted the work described in this study.

AUTHORS CONTRIBUTION

The authors acknowledge their equal contribution to every aspect of this work. All authors reviewed and approved the final version of this work.

J. Muriban (Conceptualization; Investigation; Methodology; Formal analysis; Visualisation; Writing – original draft)

R. Mamat (Supervision; Validation; Writing – Review & Editing)

G. S. Prayogo (Conceptualization; Investigation; Methodology; Writing – original draft)

M. F. Jamlos (Formal analysis; Project administration; Resources)

AVAILABILITY OF DATA AND MATERIALS

The data supporting this study's findings are available on request from the corresponding author.

ETHICS STATEMENT

Not applicable

REFERENCES

[1] J. L. Dupont, "The role of refrigeration in the global economy," International Institute of Refrigeration [Online], 2019. Available: https://iifiir.org

[2] S. S. Jose, R. K. Chidambaram, "Electric vehicle air conditioning system and its optimization for extended range - A review," *World Electric Vehicle Journal*, vol. 13, no. 11, p. 204, 2022.

[3] IEA, "World Energy Statistics and Balances," International Energy Agency [Online], 2024. Available: https://www.iea.org/data-and-statistics/data-product/world-energy-statistics-and-balances

[4] IEA, "Cooling on the Move: The Future of Air Conditioning in Vehicles," International Energy Agency [Online], 2019. Available: https://www.iea.org/reports

[5] J. Y. Kim, J. Kim, H. Jeong, G. T. Kim, J. J. Park, T. Kim, "Enhancement of electric vehicle air-conditioning system with dual condensers," *Applied Thermal Engineering*, vol. 236, p. 121459, 2024.

[6] S. S. Chaudhari, A. H. Pundkar, J. Giri, T. Sathish, A. S. Daryapurkar, R. Chadge, et al., "Optimizing air conditioning efficiency: Utilizing nano-oxides ZnO, CuO, and TiO_2 with traditional and alternative refrigerants in medium temperature range cooling systems," *Interactions*, vol. 245, no. 1, p. 108, 2024.

[7] G. S. Prayogo, R. Mamat, M. F. Ghazali, A. Nugroho, M. Kozin, J. Muriban, "A review on nanolubricant for refrigeration systems: Stability, thermophysical properties, and performance characteristics," *Mechanical Engineering for Society and Industry*, vol. 4, no. 3, pp. 388–414, 2024.

[8] I. Ahmad, Z. Said, A. K. Tiwari, "Exploring the frontier: Nanorefrigerants and nanolubricants in modern engineering," in *Nano-Refrigerants and Nano-Lubricants: Fundamentals and Applications*, pp. 1–14, 2024.

[9] A. Bhattad, J. Sarkar, "Refrigeration systems using nanorefrigerants and nanolubricants," in Nano-Refrigerants and *Nano-Lubricants: Fundamentals and Applications*, Elsevier, pp. 101–126, 2024.

[10] N. N. M. Zawawi, W. H. Azmi, M. F. Ghazali, H. M. Ali, "Performance of air-conditioning system with different nanoparticle composition ratio of hybrid nanolubricant," *Micromachines*, vol. 13, no. 11, p. 1871, 2022.

[11] M. Z. Sharif, W. H. Azmi, M. F. Ghazali, N. N. M. Zawawi, H. M. Ali, "Numerical and thermo-energy analysis of cycling in automotive air-conditioning operating with hybrid nanolubricants and R1234yf," *Numerical Heat Transfer, Part A: Applications*, vol. 83, no. 9, pp. 935–957, 2023.

[12] S. B. Cassim, A. A. Hairuddin, V. Cut, "The effects of multiwalled carbon nanotube to the performance of a refrigeration system," *Proceedings of the Institution of Mechanical Engineers, Part C: Journal of Mechanical Engineering Science*, vol. 238, no. 13, pp. 6691–6705, 2024.

[13] M. Dilawar, A. Qayoum, "Performance evaluation of novel refrigerant mixtures in an air conditioning system using Al_2O_3 nanolubricant," *Journal of Thermal Analysis and Calorimetry*, vol. 148, no. 21, pp. 11929–11943, 2023.

[14] N. N. M. Zawawi, A. H. Hamisa, W. H. Azmi, T. Y. Hendrawati, S. Safril, "Performance of hybrid electric vehicle air-conditioning using SiO_2/POE nanolubricant," *Case Studies in Thermal Engineering*, vol. 52, p. 103717, 2023.

[15] N. N. M. Zawawi, W. H. Azmi, A. H. Hamisa, T. Y. Hendrawati, A. R. M. Aminullah, "Experimental investigation of air-conditioning electrical compressor using binary TiO_2–SiO_2 polyol-ester nanolubricants," *Case Studies in Thermal Engineering*, vol. 54, p. 104045, 2024.

[16] G. El Khoury, D. Clodic, "Method of test and measurements of fuel consumption due to air conditioning operation on the new Prius II hybrid vehicle," *SAE Transactions*, vol. 114, no. 6, pp. 2563-2571, 2005.

[17] J. Lee, J. Kim, J. Park, C. Bae, "Effect of the air-conditioning system on the fuel economy in a gasoline engine vehicle," in *Proceedings of the Institution of Mechanical Engineers, Part D: Journal of Automobile Engineering*, pp. 66–77, 2013.

[18] Sanden International, "Future comfort for future cars electric compressors," Catalogue, SIEUK180062A, 2021.

[19] A. Nugroho, R. Mamat, J. Xiaoxia, Z. Bo, M. F. Jamlos, M. F. Ghazali, "Performance enhancement and optimization of residential air conditioning system in response to the novel Al_2O_3-POE nanolubricant adoption," *Heliyon*, vol. 9, p. e20333, 2023.

[20] I. M. Mahbubul, S. A. Fadhilah, R. Saidur, K. Y. Leong, M. A. Amalina, "Thermophysical properties and heat transfer performance of Al_2O_3/R-134a nanorefrigerants," *International Journal of Heat and Mass Transfer*, vol. 57, no. 1, pp. 100–108, 2013.

[21] L. S. Sundar, E. Jassim, F. Djavanroodi, "Tribological properties of nanorefrigerants and nanolubricants," in *Nano-Refrigerants and Nano-Lubricants*, Elsevier, pp. 165–188, 2024.

[22] ASHRAE, "ANSI/ASHRAE 41.9-2021 - Standard methods for refrigerant mass flow measurements using calorimeters," *American Society of Heating, Refrigerating and Air-Conditioning Engineers*, 2021.

[23] ASHRAE, "ANSI/ASHRAE 41.9-2000 (RA 2006) - Calorimeter test methods for mass flow measurements of volatile refrigerants," *American Society of Heating, Refrigerating and Air-Conditioning Engineers*, 2006.

[24] G. P. S. Daly. Automotive Air Conditioning and Climate Control Systems. 1st Ed. United Kingdom: Butterworth-Heinemann, 2006.

[25] SAE, "SAE J2765-2017 - Procedure for measuring system COP of a mobile air conditioning system on a test bench," *Society of Automotive Engineers*, 2017.

[26] ASTM International, "E230/E230M - Standard pecification and temperature-electromotive force (EMF) tables for standardized thermocouples," *American Society for Testing and Materials*, 2012.

[27] ASHRAE, "ANSI/ASHRAE Standard 41.1-1986 - Standard Method for Temperature Measurement," American Society of Heating, Refrigerating and Air-Conditioning Engineers [Online], 2006. Available: http://www.ashrae.org

[28] Y. A. Çengel, M. A. Boles. Thermodynamics: An Engineering Approach. 8th Eds. New York: McGraw-Hill, 2015.

[29] A. Kumar, A. K. Tiwari, Z. Said, "Preparation and characterization of nanorefrigerants," in *Nano-Refrigerants and Nano-Lubricants*, pp. 15–33, 2024.

[30] A. Nugroho, Z. Bo, R. Mamat, W. H. Azmi, G. Najafi, F. Khoirunnisa, "Extensive examination of sonication duration impact on stability of Al_2O_3-polyol ester nanolubricant," *International Communications in Heat and Mass Transfer*, vol. 126, p. 105418, 2021.

[31] D. C. Montgomery, G. C. Runger. Applied Statistics and Probability for Engineers. 5th Eds. United States: Wiley, 2011.

[32] Toyota, "2010 Toyota Prius Repair Manual," Technical Information [Online], 2025. Available: https://techinfo.toyota.com

[33] F. T. Knabben, A. F. Ronzoni, C. J. L. Hermes, "Effect of the refrigerant charge, expansion restriction, and compressor speed interactions on the energy performance of household refrigerators," *International Journal of Refrigeration*, vol. 130, pp. 347–355, 2021.

[34] M. Z. Sharif, W. H. Azmi, A. A. M. Redhwan, R. Mamat, T. M. Yusof, "Performance analysis of SiO_2/PAG nanolubricant in automotive air conditioning system," *International Journal of Refrigeration*, vol. 75, pp. 204–216, 2017.

[35] M. Stubblefield, J. H. Haynes. The Haynes Automotive Heating & Air Conditioning Systems Manual. 1st Ed. England: Haynes Publishing Group, 2000.

[36] M. Direk, A. Kelesoglu, A. Akin, "Drop-in performance analysis and effect of IHX for an automotive air conditioning system with R1234yf as a replacement of R134a," *Strojniški vestnik - Journal of Mechanical Engineering*, vol. 63, no. 5, pp. 314–319, 2017.

[37] J. Song, S. Lee, H. Kim, K. Park, D. J. Kim, "Experimental study of an air-conditioning system in an electric vehicle with R1234yf," *Energies*, vol. 16, no. 24, p. 8017, 2023.

[38] M. J. Akhtar, S. P. S. Rajput, "Performance analysis of ice plant using R134a/POE blended with MWCNTs nano-refrigerant – An experimental approach," *International Journal of Refrigeration*, vol. 155, pp. 333–347, 2023.